

# Fluidic Counterflow

† . † . \*

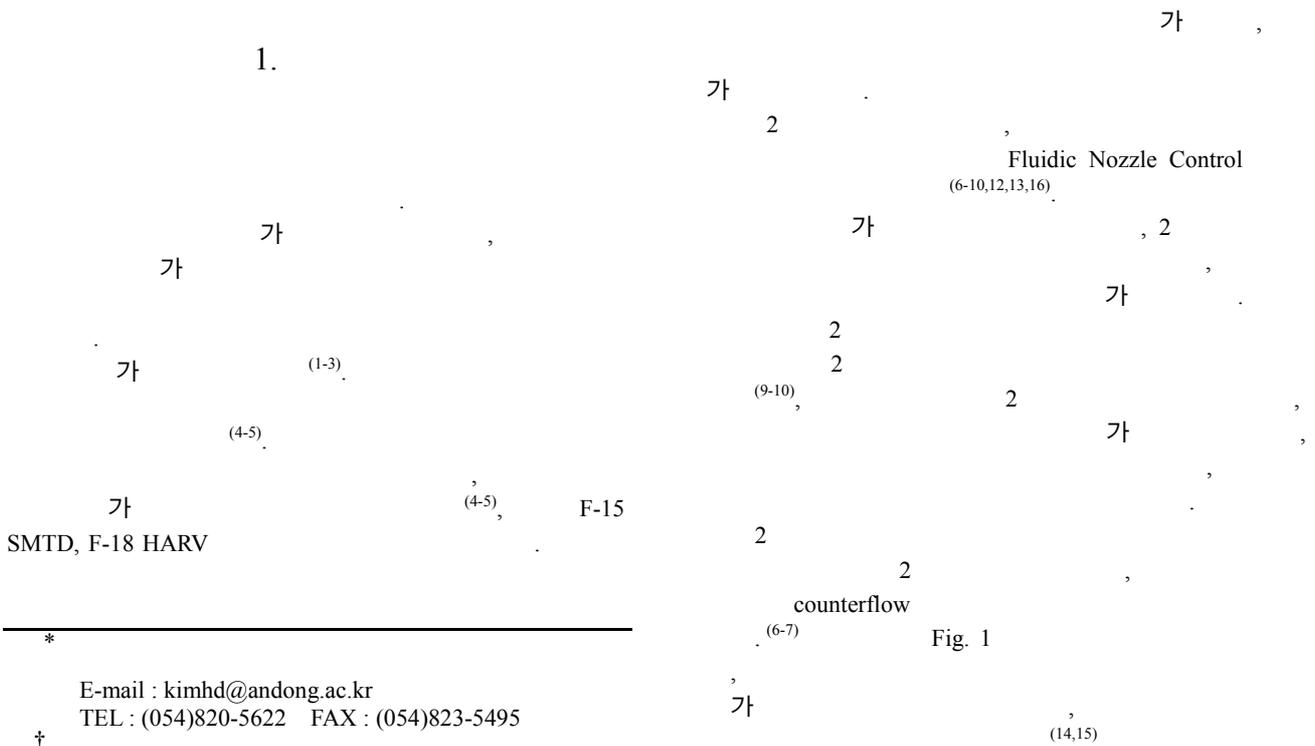
## A Study of Thrust-Vectoring Control Using Fluidic Counterflow Concept

Sung-Jae Jung, Chae-Min Lim and Heuy-Dong Kim

**Key Words :** Thrust Vector Control( ), Supersonic Nozzle( ), Supersonic Jet( ), Supersonic Ejector( ), Compressible Flow( )

### Abstract

The thrust vector control using a fluidic counterflow concept is achieved by applying a vacuum to a slot adjacent to a primary jet which is shrouded by a suction collar. The vacuum produces a secondary reverse flowing stream near the primary jet. The shear layers between the two counterflowing streams mix and entrain mass from the surrounding fluid. The presence of the collar inhibits mass entrainment and the flow near the collar accelerates causing a drop in pressure on the collar. For the vacuum asymmetrically applied to one side of the nozzle, the jet will vector toward the low-pressure region. The present study is performed to investigate the effectiveness of thrust vector control using the fluidic counterflow concept. A computational work is carried out using the two-dimensional, compressible Navier-Stokes equations, with several kinds of turbulence models. The computational results are compared with the previous experimental ones. It is found that the present fluidic counterflow concept is a viable method to vector the thrust of a propulsion system.




---

\*  
E-mail : kimhd@andong.ac.kr  
TEL : (054)820-5622 FAX : (054)823-5495  
†

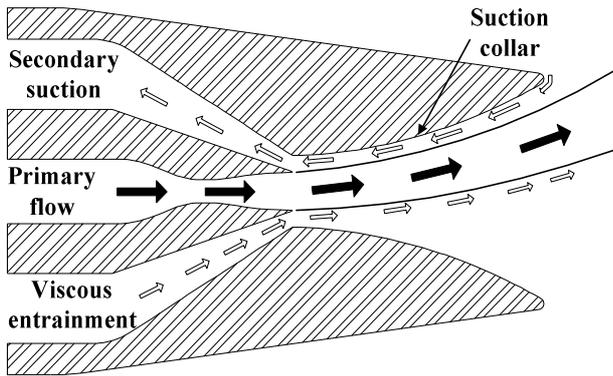


Fig. 1 Counterflow thrust vectoring concept

(2) ,  $H$   
 $H=E+p/\rho$  ,  $E$   
 $E$   
 $q$  heat flux  
 2 Navier-Stokes  
 Fluent 6  
 upwind  
 scheme, 4 Runge-Kutta  
 fluidic counterflow  
 3 가 (standard  
 $k-\epsilon$  , RNG  $k-\epsilon$  realizable  $k-\epsilon$ ) 2 가  
 (standard wall function non-equilibrium wall function)

2  
 collar  
 (entrainment) Coanda (11)  
 collar  
 가  
 2 가  
 가  
 2

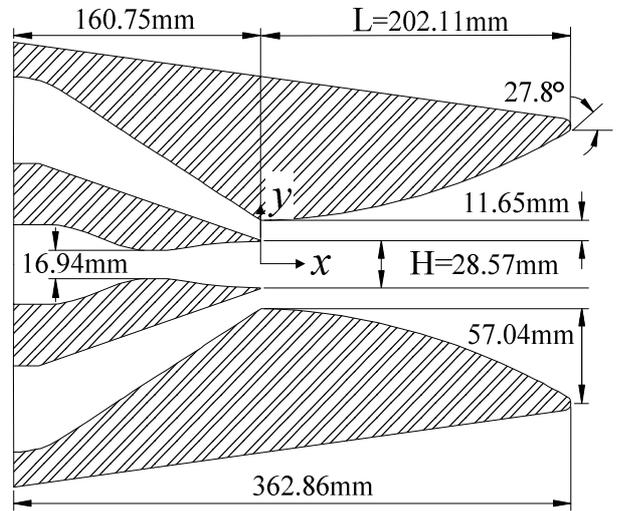


Fig. 2 Details of counterflow nozzle model

2.2

Fig. 2

2

Flamm<sup>(8)</sup>

1.62, (design NPR) 7.82  
 (design mach number) 2.0  
 114.3mm  
 1930mm<sup>2</sup>  
 slot  
 41% suction collar L 202.11mm  
 27.8°

2.3

Fig. 3

가

100  
 65000

2

2

2.1

mass averaged, time-dependent Navier-

Stokes

$V$

$$\Gamma \frac{\partial}{\partial t} \int_V Q dV + \oint [F - G] \cdot dA = 0 \quad (1)$$

$F$   $G$  viscous

flux

$Q$

$$F = \begin{bmatrix} \rho v \\ \rho v v_x + p \hat{i} \\ \rho v v_y + p \hat{j} \\ \rho v v_z + p \hat{k} \\ \rho v H \end{bmatrix}, G = \begin{bmatrix} 0 \\ \tau_{xi} \\ \tau_{yi} \\ \tau_{zi} \\ \tau_{ij} v_j + q \end{bmatrix}, Q = \begin{bmatrix} p \\ v_x \\ v_y \\ v_z \\ T \end{bmatrix} \quad (2)$$

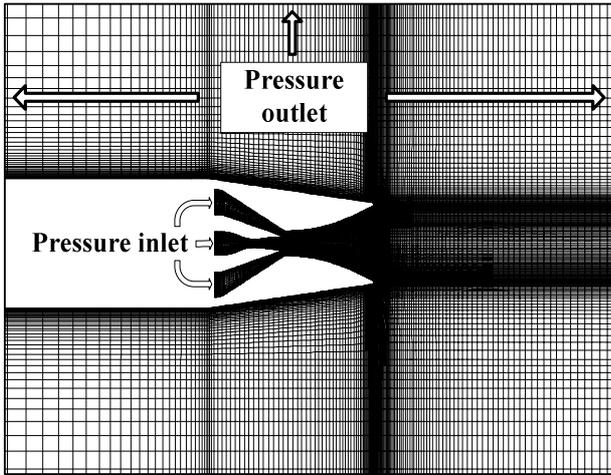


Fig. 3 Computational grid and boundary conditions

counterflow    coflow 가 ,  
 가  
 2  
 2  
 가 , pressure outlet  
 pressure inlet  
 (NPR) 8  
 2  
 pressure  
 inlet 101.325kPa 2  
 no-slip wall k  
 10<sup>-5</sup>  
 turbulent viscosity 가  
 ± 0.5%  
 Imbalance 가 0 가  
 2.4  
 fluidic counterflow  
 Hunter  
 Wing<sup>(13)</sup>  
 가  
 Fig. 4  
 p<sub>x</sub>, p<sub>y</sub> suction collar  
 suction collar x,  
 y

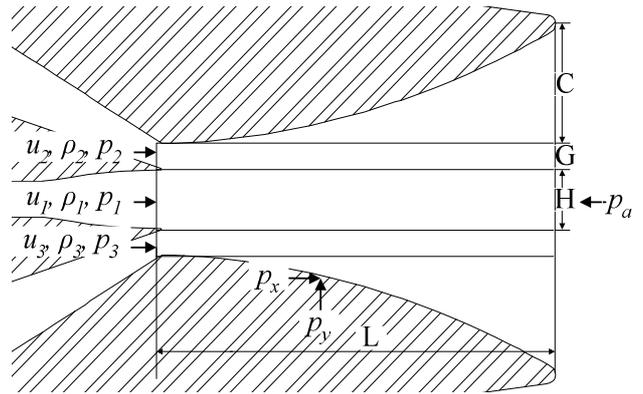


Fig. 4 Control volume analysis

$$F_a = (p_1 - p_a)HW + (p_2 - p_a)GW + (p_3 - p_a)GW + (\bar{p}_x - 2p_a)CW + \rho_1 u_1^2 HW + \rho_2 u_2^2 GW + \rho_3 u_3^2 GW \quad (4)$$

$$F_n = \bar{p}_y LW \quad (5)$$

u<sub>1</sub>, ρ<sub>1</sub>, p<sub>1</sub> , ,  
 , p<sub>2</sub> slot , p<sub>3</sub>  
 slot  
 H , G slot , C suction  
 collar , W , F<sub>n</sub> y F<sub>a</sub> x  
 , F<sub>n</sub> y (δ) (6)

$$\delta = \tan^{-1} \frac{F_n}{F_a} \quad (6)$$

(4) (5) (6) (δ<sub>cv</sub>) (7)

$$\delta_{cv} = \tan^{-1} \left( \frac{\bar{p}_y L}{p_1 H} \left[ 1 + \frac{2\gamma}{\gamma-1} \left( \frac{p_{01}}{p_1} \right)^{\frac{\gamma-1}{\gamma}} - 1 \right] + \frac{p_2}{p_1} \left[ \frac{2\gamma}{\gamma-1} \left( \frac{p_{02}}{p_2} \right)^{\frac{\gamma-1}{\gamma}} - \frac{\gamma+1}{\gamma-1} \right] \frac{G}{H} + \frac{p_3}{p_1} \left[ \frac{2\gamma}{\gamma-1} \left( \frac{p_{03}}{p_3} \right)^{\frac{\gamma-1}{\gamma}} - \frac{\gamma+1}{\gamma-1} \right] \frac{G}{H} + \frac{\bar{p}_x C}{p_1 H} - \frac{p_a H + 2G + 2C}{p_1 H} \right]^{-1} \right) \quad (7)$$

(3) pressure force momentum flux

$$\delta_{cv} \cong \tan^{-1} \left( \frac{\bar{p}_y L}{p_1 H} \left[ 1 + \frac{2\gamma}{\gamma-1} \left( \frac{p_{01}}{p_1} \right)^{\frac{\gamma-1}{\gamma}} - 1 \right] + \frac{\bar{p}_x C}{p_1 H} - \frac{p_a H + 2G + 2C}{p_1 H} \right]^{-1} \right) \quad (8)$$

, Van Der Veer<sup>(16)</sup>

Van Der Veer 가

$$\delta \propto \frac{\Delta p_{slot}}{(\gamma M^2 p)_1} \frac{L}{H} \quad (9)$$

(9) (7) (9) (7)

Van Der Veer

momentum pressure force

pressure force suction collar

suction slot

3.

Fig. 5

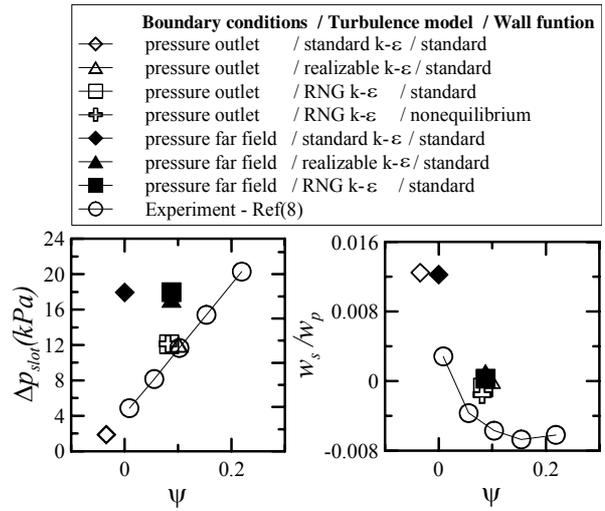


Fig. 5 Effect of computational boundary conditions

pressure outlet pressure far field (2)

standard k-ε, realizable k-ε, RNG k-ε

Fig. 4(a,b)

pressure outlet, RNG k-ε

non-equilibrium 가

Hunter Wing

counterflow (10)

$$\delta_i = \tan^{-1}(\psi) = \tan^{-1}\left(\frac{p_3 - p_2}{\rho_1 u_1^2} \frac{L}{H}\right) \quad (10)$$

slot  $p_3$  slot  $p_2$  slot

suction collar  $p_3 - p_2$

slot  $\rho_1 u_1^2$

momentum flux,  $L$  suction collar  $H$

$(p_3 - p_2)L$  suction collar

slot  $\rho_1 u_1^2 H$  normal momentum

force( $F_n$ ) axial force( $F_a$ )

flux  $\delta_i$  2 momentum flux  $\Psi$

Fig. 6 slot  $\Delta p_{slot}$   $\Psi$

$\Psi$  가 가  $\Delta p_{slot}$  가 가

$0.22 < \Psi < 0.64$   $\Delta p_{slot}$

가 suction collar

slot flamm<sup>(8)</sup>

coanda effect

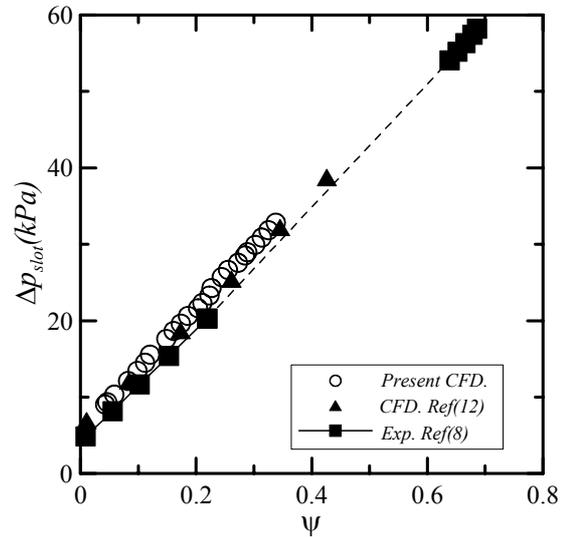


Fig. 6 Suction slot pressure correlation

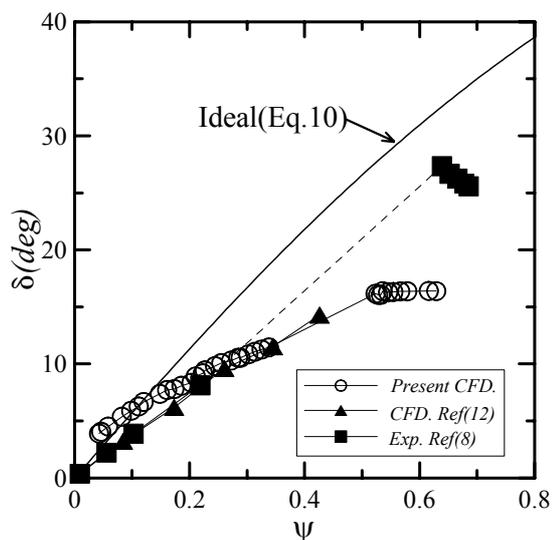


Fig. 7 Thrust vector angle

$\Delta p_{slot}$

○, ▲ Hunter<sup>(12)</sup>

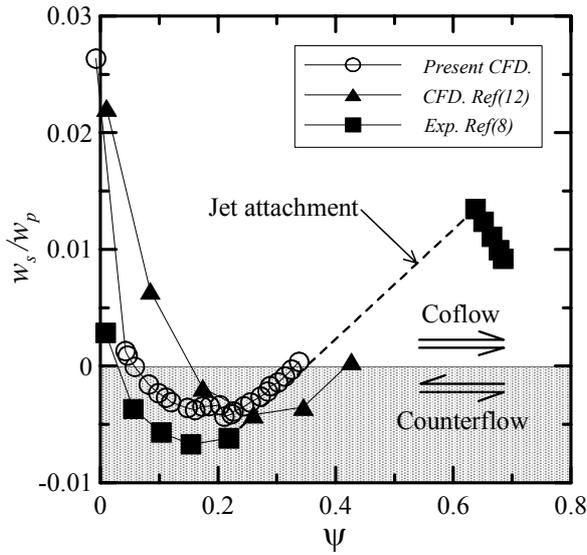


Fig. 8  $w_s/w_p$  vs  $\Psi$

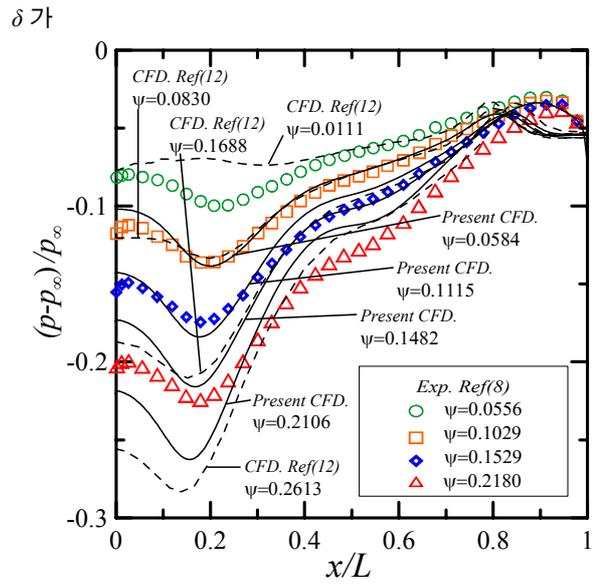
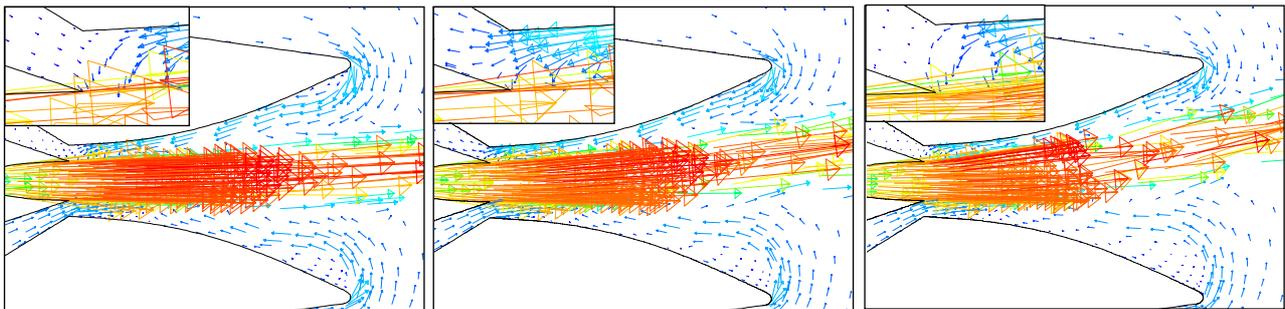


Fig. 9 Static pressure distributions on top collar surface

■ Flamm<sup>(8)</sup>  
 suction slot  
 Fig. 7  
 $\delta$   
 $\Psi$   
 (8)  
 Hunter (12)  
 Hunter  
 가  $\delta$   
 $\Psi$  가 0.22 0.64  
 $\delta$  가 8.12° 27.4° 가  $\delta=27.4^\circ$   
 suction collar  
 Flamm<sup>(8)</sup>  $\Psi=0.64$   
 suction slot  
 Hunter (12)  
 counterflow  
 NPR  
 Fig. 8  
 가 2  
 mass  
 flow ratio  
 ( $w_p$ ) 2 ( $w_s$ ) ( $w_s/w_p$ )  
 counterflow  
 coflow  $\Psi=0.009$   
 entrainment effect  
 $\Psi$  가 가  $w_s/w_p$   
 가  $\Psi$  가 가  $w_s/w_p$   
 collar  $w_s/w_p$  가  $\Psi=0.64$  가  
 Hunter (12)  
 counterflow 가 2 coflow



(a)  $\Psi=0.0425, w_s/w_p=0.00127, \delta=3.89^\circ$  (b)  $\Psi=0.2106, w_s/w_p=-0.00443, \delta=8.91^\circ$  (c)  $\Psi=0.3377, w_s/w_p=0.00035, \delta=11.45^\circ$

Fig. 10 Velocity vector contours

0.0425 <  $\Psi$  < 0.34

mass flow ratio

가 2

0.5% counterflow

Fig. 9 suction collar  
Flamm Hunter

(x) suction collar (L)

suction collar x/L 가  
x/L=0.9

가  $\Psi$  가 가  
suction collar

Fig. 10(a,b,c) 0.0425 <  $\Psi$  < 0.3377

가 suction collar  
suction collar  $\Psi$  가 가  
suction collar  
suction collar

가 Fig. 10(a)  $\Psi=0.0425$  suction collar  
entrainment  
effect  $\Psi=0.2106$   
suction slot  
Fig. 10(c)

$\Psi=0.3377$  suction slot

4.

counterflow

가

, 2

(1) counterflow

(2) 2  
suction slot  
suction collar

(3) 0.5%  
counterflow

- (1) Bitten, R. and Selmon, J., 1992, "Operational benefits of Thrust Vector Control(TVC)," High-Angle-of-Attack Technology, Vol.I, J.R. Chambers, W.P. Gilbert, and L.T. Nguyen, eds., NASA CP-3149, Part 2.
- (2) Herbst, W. B., 1980, "Future Fighter Technologies," *J. Aircraft*, Vol.17, No.8.
- (3) Herrick, P. W., 1985, "Propulsion Influences on Air Combat," AIAA-85-1457.
- (4) Bursey, R. and Dickinson, R., 1990, "Flight Test Results of the F-15 SMTD Thrust Vectoring/Thrust Reversing Exhaust Nozzle," AIAA-90-1906.
- (5) Regenie, V., Gatlin, D., Kempel, R., Matheny, N., 1992, "The F-18 High Alpha Research Vehicle: A High Angle-of-Attack Testbed Aircraft," NASA TM-104253.
- (6) Strykowski, P. J., and Krothapalli, A., 1993, "The Countercurrent Mixing Layer: Strategies for Shear-Layer Control," AIAA 93-3260.
- (7) Strykowski, P. J., Krothapalli, A. and Wishart, D., 1993, "Enhancement of Mixing in High-Speed Heated Jets Using a Counterflow Nozzle," *AIAA J.*, Vol.31, No.11.
- (8) Flamm, J. D., 1998, "Experimental Study of a Nozzle Using Fluidic Counterflow Thrust Vectoring," AIAA 98-3255.
- (9) Jung, S. J., Kim, H. D., Ahn, J. M. and Jung, D. H., 2002, "Study of the Thrust Vector Control Using a Secondary Flow Injection," Proc. KSPE Spring Annual Meeting, pp.14-15.
- (10) Green, C. J. and McCullough, M. Jr, 1963, "Liquid Injection Thrust Vector Control," *AIAA J.*, Vol.1, No.3 pp. 573-578.
- (11) Kim, H.D., Raghunathan, S., Setoguchi, T. and Matsuo, T., 2000, "Experimental and Numerical Studies of Supersonic Coanda Wall Jets," 38th Aerospace Sciences Meeting & Exhibit, AIAA-2000-0814.
- (12) Hunter, C. A. and Deere, K. A., 1999, "Computational Investigation of Fluidic Counterflow Thrust Vectoring," AIAA 99-2669.
- (13) Hunter, C. and Wing, D., 1995, "Counterflow Thrust Vectoring: Control Volume Similarity Analysis," NASA Langley Research Center White Paper.
- (14) Kim, H. D., Lee, Y. G., 1999, " Numerical Simulation of the Supersonic Flows in the Second Throat Ejector-Diffuser Systems," *J. Thermal Science*, Vol.8, No.4, pp.214-222.
- (15) Kim, H. D., Setoguchi, T., Yu, T. S. and Raghunathan, S., 1999, "Navier-Stokes Computations of the Supersonic Ejector-Diffuser System with a Second Throat," *J. Thermal Science*, Vol.8, No.2, pp.79-88.
- (16) Van Der Veer and Michael, R., 1995, "Counterflow Thrust Vectoring of a Subsonic Rectangular Jet," M. S. Thesis, University of Minnesota, Minneapolis, MN.

Hunter Wing  
counterflow (8)

$$\delta_i = \tan^{-1}(\psi) \tag{8}$$

$$\psi = \frac{p_3 - p_2}{\rho_1 U_1^2} \frac{L}{H} \tag{9}$$

slot suction collar slot suction collar slot  
 $p_3$   $p_2$   
 $\rho_1 U_1^2$   
 slot momentum flux,  $L$  suction collar,  $H$   
 $(p_3 - p_2)L$  suction collar  
 slot normal  
 force ( $F_n$ )  $\rho_1 U_1^2 H$   
 momentum flux axial force ( $F_a$ )  
 $\delta_i$  2 momentum flux  $\Psi$

$$(p_2 - p_a)GW, (p_3 - p_a)GW, \rho_2 u_2^2 GW, \rho_3 u_3^2 GW$$